Pergamon

Journal of Structural Geology, Vol. 16, No. 6, pp. 817 to 822, 1994

0191-8141/94 $07.00+0.00

Are large differential stresses required for straight fracture propagation paths?

C. E. RENSHAW and D. D. POLLARD

Department of Applied Earth Sciences, Stanford University, Stanford, CA 94305, U.S.A.

(*Received* 29 *January* 1993; *accepted in revised form* 28 *September* 1993)

Abstract—Fracture growth geometries in linear elastic materials are sensitive to the ratio between the remote differential stress, or *T*-stress, and the fracture driving stress. Two mechanically interacting fractures follow straighter paths for greater values of this ratio. We demonstrate that the degree of curvature that develops between two mechanically interacting fractures is also controlled by such factors as sub-critical fracture growth and fracture surface roughness. Sub-critical fracture growth limits the development of fracture curvature by decreasing the fracture driving stress needed for propagation. Fracture surface roughness can affect the development of fracture curvature by limiting the magnitude of the shear displacement discontinuity that can be accommodated along the fracture. Thus, propagation paths for two mechanically interacting fractures can be quite straight even in the presence of small to moderate differential stresses. Consequently, the absence of fracture curvature does not necessarily imply a high differential stress state.

INTRODUCTION

FOR over a century, geologists have attempted to relate the geometry of dominantly opening-mode fractures (i.e. joints, veins and dikes) to the ambient stress field present during their formation (see Pollard & Aydin 1988 for a discussion). Corresponding advances in our understanding of the mechanics of fracture over this time have greatly improved the methods and techniques used for these interpretations. For example, mechanical analyses have helped to relate joint and dike orientations to the existing principal stress trajectories (Ode 1957, Muller & Pollard 1977, Engelder & Geiser 1980) and to relate joint and dike dilations to driving stress magnitudes (Pollard & Muller 1976, Delaney & Pollard 1981, Segall & Pollard 1983). A better understanding of the relationship between stress state and fracture geometry is critical to our further understanding of geologic fracture problems.

It is well known that when fractures grow under conditions of mixed-mode I–II loading ($K_{III} = 0$), the paths of the fractures are often curved or kinked (Lawn & Wilshaw 1975). Analyses based on linear elastic fracture mechanics have shown that smoothly curved fracture paths in non-uniform stress fields are such that the mode II stress intensity factor is minimized (Goldstein & Salganik 1974, Cotterell & Rice 1980). In particular, as the remote differential stress decreases, fracture propagation paths for mechanically interacting fractures become more curvaceous. Consequently, it has been suggested that fracture interaction geometries in homogeneous and isotropic materials are indicative of the ambient stress state present during fracture formation (Olson & Pollard 1989, Cruikshank *et al.* 1991, Thomas & Pollard 1993).

In this paper, we explore the following question: if a relatively straight fracture propagation path is observed for two mechanically interacting fractures in a homogenous and isotropic rock mass, does this necessarily indicate that a large differential stress existed during propagation? Or could other factors result in straight propagation paths even in the presence of small to moderate differential stresses?

BACKGROUND

We restrict our attention to two-dimensional fractures subject to in-plane (modes I and II) loadings. If the material is homogeneous and isotropic, pure-mode I (opening) fractures will be oriented perpendicular to σ_1^r, the greatest remote tensile stress (Stevens 1911, Ode 1957, Anderson 1972, Lawn & Wilshaw 1975). The smoothly curving path taken by a completely open fracture will be such that mode II (shear) loading near the fracture tip is minimized (Cotterell & Rice 1980). This result, known as the *criterion of local symmetry* (Goldstein & Salganik 1974), is consistent with the various mixed-mode propagation criteria proposed in the literature in that all these criteria predict abrupt changes (kinks) in the fracture path whenever $K_{II} \neq 0$ (Erdogan & Sih 1963, Hussain *et al.* 1974, Sih 1974). In particular, since $K_{II} = 0$ for any isolated planar fracture oriented parallel to a principal stress direction, the propagation path of the fracture shown in Fig. 1(a) in a perfectly homogeneous material will be a straight line parallel to the x_3-axis.

Local stress perturbations

As real materials are not perfectly homogeneous, local heterogeneities induce shear stresses and shear

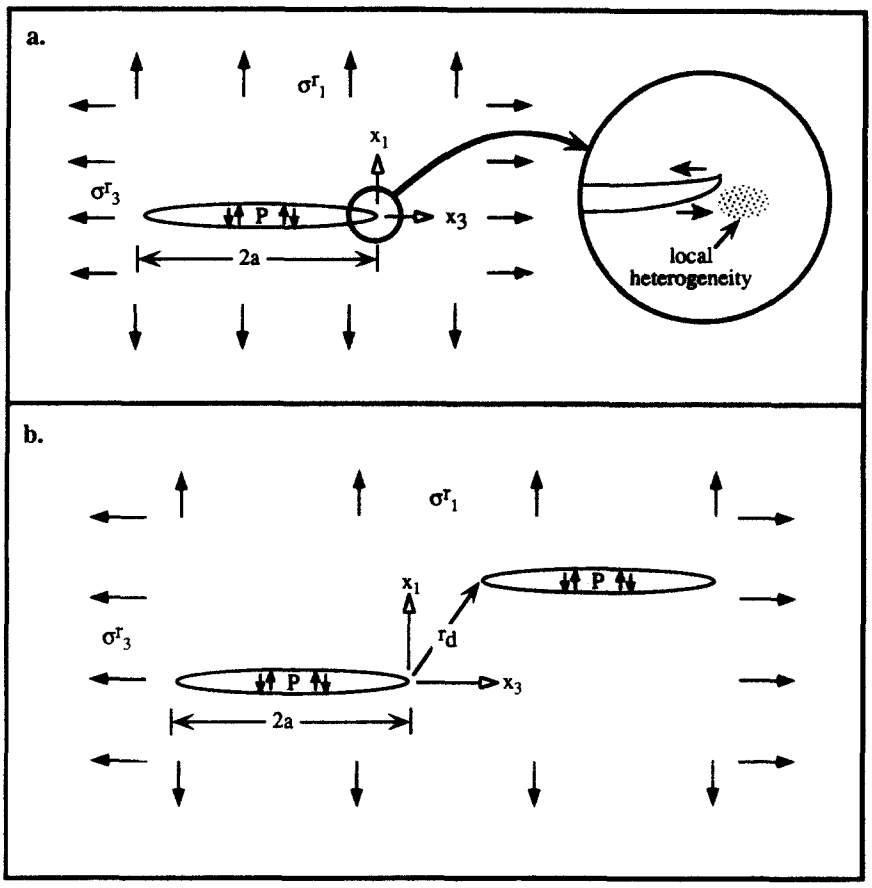

Fig. 1. (a) Co-ordinate system used to define the T-stress and stress ratio R. Inset demonstrates how a local heterogeneity can alter the propagation path. (b) Co-ordinate system used to describe the interactions between two fractures arranged in an echelon geometry.

displacement discontinuities at actual fracture tips ($K_{II} \neq 0$), causing propagation to deviate from a straight path (Fig. 1a—inset). Whether the deviated fracture tip returns to the projected straight path or continues to deviate will depend upon the stability of the straight propagation path, which is controlled by the *transverse* or 'T'-stress (Cotterell 1966, Cotterell & Rice 1980). For the fracture shown in Fig. 1(a), the T-stress is defined as:

$$T = (\sigma^r_3 - \sigma^r_1), \tag{1}$$

where σ^r_1 (σ^r_3) is the greatest (least) remote principal stress and tension is positive.

Since a deviated fracture tip is no longer parallel to the direction of the remote principal stress, the T-stress induces a shear displacement discontinuity at the fracture tip. If $T > 0$, the shearing induced by the T-stress will be of the same sign as that induced by the local heterogeneity. Hence, the sign of the K_{II} induced by the T-stress will be the same as that induced by the heterogeneity and the fracture path will continue to curve. Thus when $T > 0$, the straight fracture propagation path is *unstable*.

If $T < 0$, the shearing induced by the T-stress will be in the opposite sense to that induced by the local heterogeneity and the signs of the respective K_{II}s will be different. When the magnitude of K_{II} induced by the T-stress is much greater than the magnitude of the K_{II} induced by the local heterogeneity, the fracture will return to the straight path. Therefore whenever $T < 0$ and the magnitude of T is much greater than the magnitude of the local stress perturbation, the straight fracture propagation path is *stable*.

Common sources of heterogeneity in a rock mass are other fractures. When the spacing between two fractures approaches the length of the larger fracture, their mechanical interaction will induce non-uniform, mixed-mode loading, possibly resulting in curved propagation paths (Swain & Hagan 1978, Pollard *et al.* 1982, Sempere & Macdonald 1986, Fleck 1991). For two mechanically interacting fractures arranged in an echelon geometry (Fig. 1b), the magnitude of the stress perturbation at one fracture due to the presence of a second fracture can be expressed as an *interaction* or 'I'-stress:

$$I = C_g(\sigma^r_1 + P), \tag{2}$$

where C_g depends only on the geometry of the fractures and ($\sigma^r_1 + P$) is the *driving stress* of the second fracture. For fractures of length $2a$, where the distance between the inner fracture tips is equal to r_d (Fig. 1b), it can be shown (e.g. Du & Aydin 1991) that for very close spacing ($r_d \ll a$), the maximum value of C_g is on the order of:

$$C_g \approx O\left[\sqrt{\frac{a}{r_d}}\right], \tag{3}$$

where $O[]$ indicates the order of magnitude. For very

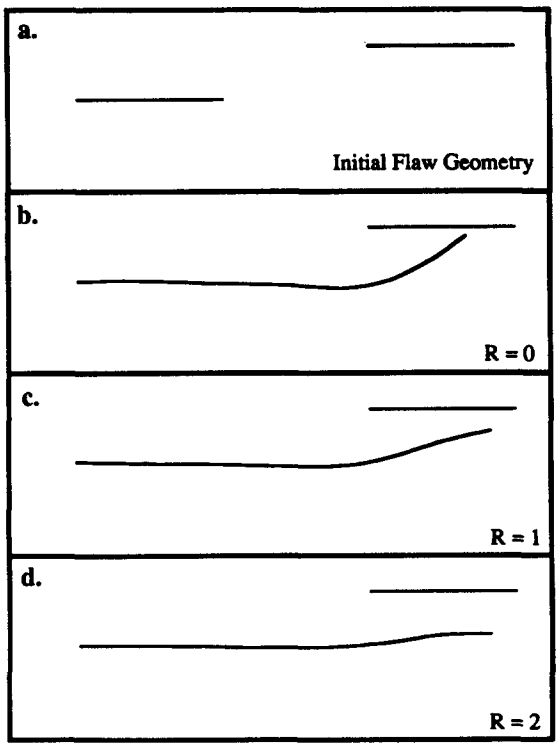

Fig. 2. Sensitivity of fracture paths to the stress ratio R. Two initial flaws were of equal length and arranged as shown in (a). Only the inner right fracture tip of the lower fracture was allowed to propagate.

wide spacing ($r_d > 1.5a$), the maximum value of C_g is on the order of:

$$C_g \approx O\left[\left(\frac{a}{r_d}\right)^2\right]. \tag{4}$$

For intermediate spacing, C_g can be determined numerically (e.g. Thomas & Pollard 1993).

Unlike the T-stress which is constant for a given loading, the I-stress varies continuously as the fracture propagates. This precludes the derivation of a simple stability criterion for straight paths. However, as for an isolated fracture, if $T > 0$, the shearing induced by the T-stress at the tips of the interacting fractures will be in same direction as that induced by I-stress and the straight path will be unstable. If $T < 0$, the stability of the straight path will depend on the relative magnitudes of the T- stress and the I-stress.

For example, consider a given initial fracture geometry (e.g. Fig. 2a) where the fractures are oriented parallel to the principal stresses and where the geometry varies only in two dimensions. For a range of loadings that are both sufficient for propagation to occur and such that $T < 0$, the tendency for straight propagation is quantified by the ratio R (Cruikshank *et al.* 1991).

$$R = \frac{-T}{(\sigma_1^r + P)} = \frac{(\sigma_1^r - \sigma_3^r)}{(\sigma_1^r + P)}, \tag{5}$$

where $\sigma_1^r - \sigma_3^r$ is the remote *differential stress*. A similar ratio between the remote differential stress and an average fracture driving stress for mixed-mode I–III loadings is discussed by Pollard *et al.* (1982).

Figure 2 demonstrates the effect that varying stress ratios R have on fracture paths for two mechanically interacting open fractures propagating towards each other in an infinite homogeneous isotropic linear elastic medium. Fracture paths were calculated using a boundary element method similar to Olson & Pollard (1989, 1991). Comparable fracture paths have been simulated experimentally on acrylic sheets (Thomas & Pollard 1993). When the stress ratio is zero, stress perturbations caused by mechanical interaction control the propagation path. As the stress ratio increases, the T-stress becomes large in comparison to the I-stress and propagation path becomes straighter.

Regional stress fields during propagation

In geologic settings, σ_1^r and σ_3^r are typically compressive (negative). Thus the internal fluid pressure P must be large enough to overcome the magnitude of the minimum compressive stress and to increase the driving stress of the initial flaw to the point where it begins to propagate. In particular, if S_h (S_H) is the minimum (maximum) principal compressive stress:

$$\sigma_1^r = -S_h$$
$$\sigma_3^r = -S_H. \tag{6}$$

Then, for an isolated fracture with a length of $2a$, the magnitude of P at propagation must be (e.g. Broek 1986)

$$P = S_h + \frac{K_{Ic}}{\sqrt{\pi a}}, \tag{7}$$

where K_{Ic} is the mode I critical stress intensity factor (fracture toughness) for the material. Combining equations (5)–(7), the expression for the stress ratio R can be rewritten as:

$$R = \frac{\sqrt{\pi a}(S_H - S_h)}{K_{Ic}}. \tag{8}$$

For any particular formation, equation (8) allows values of the stress ratio R to be estimated from investigations of *in situ* stress states and the fracture properties of the geologic material.

For example, field measurements of the state of stress in the Earth's crust (typically based on information from wellbore breakouts, hydraulic fracturing and/or seismic focal mechanisms) suggest that at depths less than 4 km the differential stress often is within the range (McGarr & Gay 1978, Barton *et al.* 1988, Cornet & Julien 1989, Guenot 1989, Hayashi *et al.* 1989, Ljunggren & Amadei 1989, Matsunaga *et al.* 1989):

$$0 \leq (S_H - S_h) \leq 40 \text{ MPa}. \tag{9}$$

Similarly, a typical range of the critical stress intensity factor K_{Ic} can be derived from published stress intensity factor measurements collated by Atkinson & Meredith (1987b). For many rock types at moderate temperatures and confining pressures:

$$0.35 \leq K_{Ic} \leq 3.5 \text{ MPa} \cdot \text{m}^{1/2}. \tag{10}$$

While K_{Ic} values are known to increase with increasing fracture length for fractures subject to plane-stress boundary conditions (Broek 1986), these boundary conditions rarely, if ever, exist in geologic environments.

Substituting the parameter ranges in (9)–(10) into equation (8) suggests that for fractures of length $2a$ m within 4 km of the surface, typical values of the stress ratio are within the range:

$$0 \leq R \leq 200\sqrt{a}. \tag{11}$$

For example, the R value for a 1 m long fracture ranges between 0 and approximately 140, while for a 10 m long fracture, R values range between 0 and 450. While different assumptions concerning the appropriate value for K_{Ic} may increase or decrease the maximum value for R given in equation (11), we suggest that expected values of R range between 0 and something on the order of a few tens to a few hundreds.

We conclude that some natural fractures have roughly planar geometries due to the occurrence of large differential stresses which limit the development of fracture curvature. Other fractures which develop under relatively small differential stresses may be quite curvaceous. However, in what follows we argue that the development of fracture curvature may be limited even in the presence of a low differential stress. Thus while curvaceous patterns accurately reflect low differential stress states, their absence does not automatically imply the presence of a high differential stress state.

SUB-CRITICAL FRACTURE GROWTH

In writing equation (7), we have assumed that fracture growth is dynamic and that no fracture growth occurs when $K_I < K_{Ic}$. However, it is well known that fracture growth can occur even when $K_I < K_{Ic}$ by means of sub-critical growth mechanisms such as chemical stress corrosion (Swanson 1984, Atkinson & Meredith 1987b). Indeed, in the saturated environments subject to long-term loadings which are often found in the Earth's crust, sub-critical fracture growth mechanisms such as chemical stress corrosion may be the dominate mechanism for fracture growth. If fracture growth is due to chemical stress corrosion, then equation (7) needs to be rewritten as:

$$P = S_h + \frac{K^*}{\sqrt{\pi a}}, \tag{12}$$

where K^* is the stress intensity factor. For sub-critical fracture growth to occur, K^* must be in the range:

$$K_o \leq K^* \leq K_{Ic} \tag{13}$$

where K_o is the stress corrosion limit (Atkinson 1984).

Using equation (12), the stress ratio R for sub-critical fracture growth can be written as:

$$R = \frac{\sqrt{\pi a}(S_H - S_h)}{K^*}. \tag{14}$$

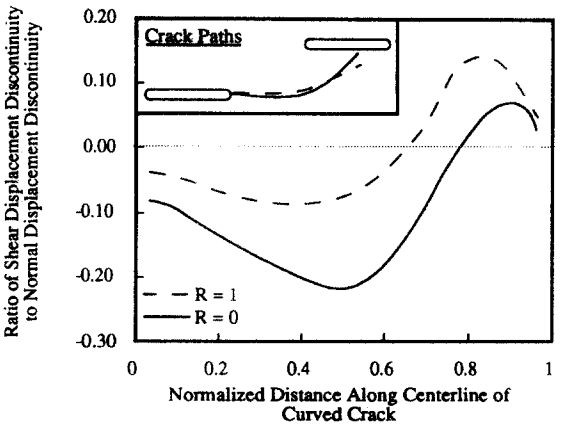

Fig. 3. Ratio of shear to normal displacement discontinuity along two curved fractures. The displacement discontinuity represents the distance between two originally adjacent points on either side of the fracture. The two fracture paths were modeled under uniform tension ($R = 0$) and uniaxial tension ($R = 1$) and are the same solutions as in Figs. 2(b) & (c).

As $K^* < K_{Ic}$, a comparison between equations (8) and (14) suggests that the stress ratio R for a fracture growing via chemical stress corrosion will be larger than that for a fracture that only grows when $K_I = K_{Ic}$. Further, since K^* is often much less than K_{Ic} and can be quite small (indeed, a lower bound for K_o has yet to be identified (Atkinson & Meredith 1987a)), the stress ratio R can be quite large even when the differential stress is small. Consequently, propagation paths for two mechanically interacting fractures growing sub-critically can be quite straight even under small to moderate differential stresses.

A NEW CURVATURE LIMITING MECHANISM

Clearly, any significant anisotropy in material strength will limit the development of fracture curvature regardless of the magnitude of the differential stress. However, even in isotropic, homogeneous media, the development of fracture curvature depends on more than just the stress state. For example, in this section we demonstrate that fracture surface roughness can strongly influence the propagation paths of interacting fractures.

We demonstrate the influence of fracture surface roughness on propagation paths by first noting that stresses at a fracture tip depend on the relative motion of the fracture walls (i.e. the displacement discontinuity) along the entire fracture. As such, it is important to consider conditions along the entire fracture surface when analyzing fracture propagation. For example, Fig. 3 is a plot of the ratio of shear to normal displacement discontinuities along the two curved fracture paths shown in the inset. These are the same solutions illustrated in Figs. 2(b) & (c). Note that for both fractures, the magnitude of the shear displacement discontinuity ranges up to more than 10% of the normal displacement discontinuity. A question thus arises as to what happens if the shear displacement discontinuity along the frac-

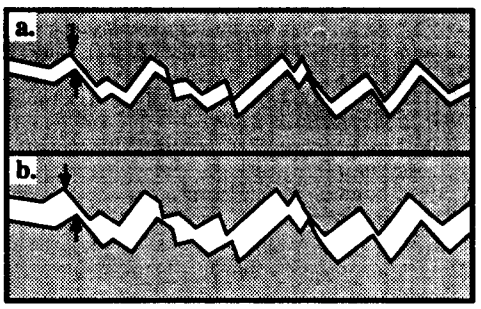

Fig. 4. Two hypothetical rough fracture wall surfaces. Arrows indicate the magnitudes of the normal and shear displacement discontinuities. Note how the maximum magnitude of shear displacement discontinuity accommodated at this interface is related to the amount of normal displacement.

ture surface cannot be accommodated? Would this alter the fracture path?

For example, consider the hypothetical fracture surfaces shown in Figs. 4(a) & (b). The amount of shear displacement discontinuity that can be accommodated along this interface is a function of the normal (opening) displacement discontinuity; the more opening, the more shear displacement discontinuity that can be accommodated. As natural fracture surfaces in rock have roughness due to grain boundaries and growth features such as hackle marks and hesitation lines (Brown & Scholz 1985, Brown *et al.* 1986, Power *et al.* 1987, Pollard & Aydin 1988), the amount of shear displacement discontinuity that a natural fracture can accommodate also is related to the amount of normal displacement discontinuity. Similar concerns about accommodation of the shear displacement discontinuity along rough fracture surfaces and its influence on fracture propagation have been raised by several investigators studying fracture propagation in laboratory specimens (Hussain *et al.* 1974, Kenner *et al.* 1982, Swanson 1987).

The boundary element fracture propagation model (Olson & Pollard 1989, 1991) was used to investigate the influence of limited shear accommodation on propagation paths by assuming that the magnitude of the shear displacement discontinuity at every point along the fracture could only be less than or equal to some constant fraction of the normal displacement/discontinuity magnitude at that location. If the calculated shear displacement discontinuity at the midpoint of any element exceeded the maximum allowable, the magnitude of the shear displacement discontinuity at that element was adjusted downward to the maximum allowable, and the normal and shear displacement discontinuities at all the elements recalculated. This process was repeated until the maximum allowable shear displacement discontinuity was not exceeded at any element.

Figure 5 shows the resulting fracture paths for a fracture propagating toward a second echelon fracture. The initial geometry of the two fractures is the same as in Fig. 2 and the fractures are subject to uniform remote tension ($R = 0$). When the maximum allowable ratio of shear (S) to normal (N) displacement discontinuity along the fracture is large ($S/N \leq 0.15$), the propagation path is equivalent to the case with no restriction on the

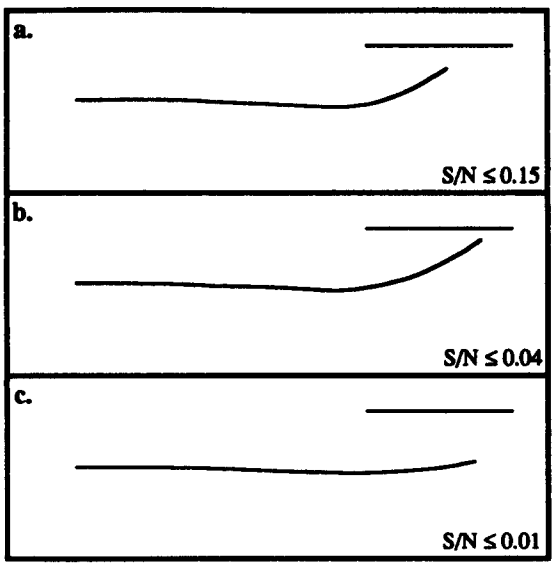

Fig. 5. Fracture paths for various maximum shear (S) to normal (N) discontinuity ratios. Initial flaw geometry and the remote differential stress are the same as for Fig. 2(b).

amount of shear displacement discontinuity (cf. Figs. 2b and 5a). However, as the maximum allowable ratio of shear to normal displacement discontinuity is decreased ($S/N \leq 0.04$ and $S/N \leq 0.01$), the propagation path becomes straighter (Figs. 5b & c).

DISCUSSION AND CONCLUSIONS

We have demonstrated how the degree of fracture curvature that develops between two mechanically interacting fractures depends not only upon the remote differential stress, but also upon such factors as the growth mechanism and the fracture surface roughness. It has been shown by others that the slower growth rates often associated with sub-critical fracture growth lead to a more inter-granular (as opposed to trans-granular) fracturing (Meredith & Atkinson 1983, Hatton *et al.* 1993). As inter-granular fracturing results in rougher fracture surfaces than trans-granular fracturing, fracture growth in the sub-critical regime may enhance the influence of fracture surface roughness on propagation paths.

Other factors may also strongly influence fracture interaction geometries. For example, it has been shown that fracture interactions are generally weaker in three-dimensional configurations than in two-dimensional configurations (Kachanov 1987). Similarly, the interaction between natural hydraulic fractures, where the build up of fluid pressure within the fracture is limited by fluid diffusion from the surrounding rock matrix (Secor 1965, 1969), is weaker than the interaction between fractures having constant internal fluid pressures.

Since fracture interaction geometries depend upon more than just the remote differential stress, it may be dangerous to use the results from numerical models of fracture propagation that ignore these curvature-limiting and other, possibly curvature-enhancing, mech-

anisms. Consequently, predictions of the *absolute magnitude* of the differential stress during the formation of a fracture set should be reviewed with skepticism unless all of the curvature-influencing mechanisms have been evaluated.

In many situations it may be reasonable to assume that the factors controlling fracture curvature, other than the stress state, were similar for two different fracture sets. In these cases, comparisons between the *relative magnitudes* of the differential stress during the formation of both sets can reasonably be made (Olson & Pollard 1989, Cruikshank *et al.* 1991). However, comparisons between fracture sets from different fracture networks, particularly between fracture sets from different rock types and/or different geologic settings, may be problematic.

Acknowledgements—We wish to thank J. R. Rice and P. G. Meredith for their careful reviews and numerous helpful comments. This material is based upon work supported under a National Science Foundation Graduate Fellowship. Additional support was provided by the U.S. Department of Energy (EAR-8903631), the U.S. National Science Foundation (BCS-8957186) and the Stanford Rock Fracture Project. Computer equipment used for this work was provided by the Hewlett-Packard Company.

REFERENCES

Anderson, E. M. 1972. *The Dynamics of Faulting*. Hafner, New York.

Atkinson, B. K. 1984. Subcritical crack growth in geological materials. *J. geophys. Res.* **89**, 4077–4114.

Atkinson, B. K. & Meredith, P. G. 1987a. The theory of subcritical crack growth with applications to minerals and rocks. In: *Fracture Mechanics of Rock* (edited by Atkinson, B. K.). Academic Press, London, 111–166.

Atkinson, B. K. & Meredith P. G. 1987b. Experimental fracture mechanics data for rocks and minerals. In: *Fracture Mechanics of Rock* (edited by Atkinson, B. K.). Academic Press, London, 477–525.

Barton, C. A., Zoback, M. D. & Burns, K. L. 1988. In-situ stress orientation and magnitude at the Fenton geothermal site, New Mexico, determined from wellbore breakouts. *Geophys. Res. Lett.* **15**, 467–470.

Broek, D. 1986. *Elementary Engineering Fracture Mechanics*. Martinus Nijhoff, Boston.

Brown, S. R., Kranz, R. L. & Bonner, B. P. 1986. Correlation between the surfaces of natural rock. *Geophys. Res. Lett.* **13**, 1430–1433.

Brown, S. R. & Scholz, C. H. 1985. Broad bandwidth study of the topography of natural rock surfaces. *J. geophys. Res.* **90**, 12,575–12,582.

Cornet, F. H. & Julien, P. H. 1989. Stress determination from hydraulic test data and focal mechanisms of induced seismicity. *Int. J. Rock Mech. Min. Sci. & Geomech. Abs.* **26**, 235–248.

Cotterell, B. 1966. Notes on the paths and stability of cracks. *Int. J. Fract. Mech.* **2**, 526–533.

Cotterell, B. & Rice, J. R. 1980. Slightly curved or kinked cracks. *Int. J. Fract.* **16**, 155–169.

Cruikshank, K. M., Zhao, G. & Johnson, A. M. 1991. Analysis of minor fractures associated with joints and faulted joints. *J. Struct. Geol.* **13**, 865–886.

Delaney, P. T. & Pollard, D. D. 1981. Deformation of host rocks and flow of magma during growth of minette dikes and breccia-bearing intrusions near Ship Rock, New Mexico. *Prof. Pap. U.S. geol. Surv.* **1202**.

Du, Y. & Aydin, A. 1991. Interaction of multiple cracks and formation of echelon crack arrays. *Int. J. Num. Anal. Meth. Geomech.* **15**, 205–218.

Engelder, T. & Geiser, P. 1980. On the use of regional joint sets as trajectories of paleostress fields during the development of the Appalachian Plateau, New York. *J. geophys. Res.* **85**, 6319–6341.

Erdogan, F. & Sih, G. C. 1963. On the crack extension in plates under in plane loading and transverse shear. *J. Basic Engng ASME* **85**, 519–527.

Fleck, N. A. 1991. Brittle fracture due to an array of microcracks. *Proc. R. Soc. Lond.* **A432**, 55–76.

Goldstein, R. V. & Salganik, R. L. 1974. Brittle fracture of solids with arbitrary cracks. *Int. J. Frac.* **10**, 507–523.

Guenot, A. 1989. Borehole breakouts and stress fields. *Int. J. Rock Mech. Min. Sci. & Geomech. Abs.* **26**, 185–195.

Hatton, C. G., Main, I. G. & Meredith, P. G. 1993. A comparison of seismic and structural measurements of fractal dimension during tensile subcritical crack growth. *J. Struct. Geol.* **15**, 1485–1495.

Hayashi, K., Ito, I. & Abe, H. 1989. In situ stress determination by hydraulic fracturing—A method employing an artificial notch. *Int. J. Rock Mech. Min. Sci. & Geomech. Abs.* **26**, 197–202.

Hussain, M. A., Pu, S. L. & Underwood, J. H. 1974. Strain energy release rate for a crack under combined Mode I and Mode II. *Fract. Anal. ASTM STP* **560**, 2–28.

Kachanov, M. 1987. Elastic solids with many cracks: A simple method of analysis. *Int. J. Solids. Struct.* **23**, 23–43.

Kenner, V. H., Advani, S. H. & Richard, T. G. 1982. A study of fracture toughness for an anisotropic shale. *Proc. 23rd U.S. Symp. on Rock Mechanics, Berkeley* **23**, 471–479.

Lawn, B. R. & Wilshaw, T. R. 1975. *Fracture of Brittle Solids*. Cambridge University Press, Cambridge, 66–72.

Ljunggren, C. & Amadei, B. 1989. Estimation of virgin rock stresses from horizontal hydrofractures. *Int. J. Rock Mech. Min. Sci. & Geomech. Abs.* **26**, 69–78.

Matsunaga, I., Kuriyagawa, M. & Sasaki, S. 1989. In situ stress measurements by the hydraulic fracturing method at Imaichi pumped storage power plant, Tochigi, Japan. *Int. J. Rock Mech. Min. Sci. & Geomech. Abs.* **26** 203–209.

McGarr, A. & Gay, N. C. 1978. State of stress in the earth's crust. *Annu. Rev. Earth Planet. Sci.* **6**, 405–436.

Meredith, P. G. & Atkinson, B. K. 1983. Stress corrosion and acoustic emission during tensile crack propagation in Whin Sill dolerite and other basic rocks. *Geophys. J. R. astr. Soc.* **75**, 1–21.

Muller, O. H. & Pollard, D. D. 1977. The stress state near Spanish Peaks, Colorado, determined from a dike pattern. *Pure & Appl. Geophys.* **115**, 69–86.

Ode, H. 1957. Mechanical analysis of the dike pattern of the Spanish Peaks area, Colorado. *Bull. geol. Soc. Am.* **68**, 567–576.

Olson, J. & Pollard, D. D. 1989. Inferring paleostresses from natural fracture patterns: A new method. *Geology* **17**, 345–348.

Olson, J. O. & Pollard, D. D. 1991. The initiation and growth of en échelon veins. *J. Struct. Geol.* **13**, 595–608.

Pollard, D. D. & Aydin, A. 1988. Progress in understanding jointing over the past century. *Bull. geol. Soc. Am.* **100**, 1181–1204.

Pollard, D. D. & Muller, O. H. 1976. The effect of gradients in regional stress and magma pressure on the form of sheet intrusions on cross section. *J. geophys. Res.* **81**, 975–988.

Pollard, D. D., Segall P. & Delaney, P. T. 1982. Formation and interpretation of dilatant echelon cracks. *Bull. geol. Soc. Am.* **93**, 1291–1303.

Power, W. L., Tullis, T. E., Brown, S. R., Boitnott, G. N. & Scholz, C. H. 1987. Roughness of natural fault surfaces. *Geophys. Res. Lett.* **14**, 29–32.

Secor, D. T. 1965. Role of fluid pressure in jointing. *Am. J. Sci.* **263**, 633–646.

Secor, D. T. 1969. Mechanics of natural extension fracturing at depth in the earth's crust. *Geol. Surv. Can. Pap.* **68-52**, 3–48.

Segall, P. & Pollard, D. D. 1983. Joint formation in granitic rock of the Sierra Nevada. *Bull. geol. Soc. Am.* **94**, 563–575.

Sempere, J. C. & Macdonald, K. C. 1986. Overlapping spreading centers: Implications from crack growth simulation by the displacement discontinuity method. *Tectonics* **5**, 151–163.

Sih, G. C. 1974. Strain-energy-density factor applied to mixed-mode crack problems. *Int. J. Fracture Mech.* **10**, 305–321.

Stevens, B. 1911. The laws of Intrusion. *Am. Inst. Min. Metall. Engr. Trans.* **49B**, 1–23.

Swain, M. V. & Hagan, J. T. 1978. Some observations of overlapping interacting cracks. *Engng Fract. Mech.* **10**, 299–304.

Swanson, P. L. 1984. Subcritical crack growth and other time- and environment-dependent behavior in crustal rocks. *J. geophys. Res.* **89**, 4137–4152.

Swanson, P. L. 1987. Tensile fracture resistance mechanisms in brittle polycrystals: An ultrasonics and in situ microscopy investigation. *J. geophys. Res.* **92**, 8015–8036.

Thomas, A. L. & Pollard, D. D. 1993. The geometry of echelon fractures in rock: Implications from laboratory and numerical experiments. *J. Struct. Geol.* **15**, 323–334.